Journal of ELECTRONIC MATERIALS, Vol. 45, No. 7, 2016
DOI: 10.1007/s11664-016-4470-0

Compositional Dependence of the Optical Properties of Amorphous Semiconducting Glass $Se_{80}Ge_{20-x}Cd_x$ ($0 \le x \le 12$ at.%) Thin Films

N.A. HEGAB,[1] A.S. FARID,[1] A.M. SHAKRA,[1] M.A. AFIFI,[1] and A.M. ALREBATI[1,2,3]

1.—Physics Department, Semiconductor Lab, Faculty of Education, Ain Shams University, Cairo, Egypt. 2.—Physics Department, Faculty of Education, Taiz University, Taiz, Yemen. 3.—e-mail: alribaty@yahoo.com

$Se_{80}Ge_{20-x}Cd_x$ ($0 \le x \le 12$ at.%) compositions were prepared by a quenching technique. Thin films of the obtained compositions were deposited on dry clean glass substrates by a thermal evaporation technique. The chemical composition of the film samples have been determined by energy dispersive x-ray spectroscopy (EDX). X-ray diffraction measurements showed the amorphous nature of the studied films. The optical constants (n, k) were determined for the studied films using spectrophotometric measurements of transmittance $T(\lambda)$ in the wavelength range (350 nm to 2500 nm), and using Swanepoel's method. The values of the dispersion energy E_d, oscillator energy E_o, the lattice dielectric constant $\varepsilon_{\infty L}$ and the high-frequency dielectric constant ε_s were determined. The optical band gap E_g^{opt} is estimated for all compositions from the absorption coefficient α. The analysis of the optical absorption data revealed the existence of allowed indirect transitions for all compositions. The effect of adding Cd content on the obtained optical parameters was also discussed.

Key words: Chalcogenide glasses, optical properties, Se-Ge-Cd

INTRODUCTION

Amorphous semiconductors, in particular chalcogenide glasses, are a recognized group of inorganic glass materials, which always contain one or more of the chalcogen elements (e.g., Se, S or Te) as a main constituent.[1,2] In recent years, the optical memory effects in chalcogenide have been investigated and used for fabrication of various technological applications. Diverse studies of the optical properties of amorphous chalcogenide glasses have been done for many reasons such as the use of these materials in optical fibers, reflective coatings, optical recording and integrated optics such as all optical switches, gratings and waveguides.[3–7] Impurity effects in chalcogenide glasses have a great importance in fabrication of glass semiconductors. Some impurities are added to chalcogenide glasses to modify thermal, mechanical, electrical and optical properties which enable the development of new materials with high quality for device industry. Different factors affect the roles of impurity atoms in chalcogenide glasses, which is related to the composition of the glass, and the chemical nature and concentration of the impurity atoms. Several studies[8–11] reported the impurity effect in various chalcogenide glasses. For example, the investigation of Ge-Se-Cd film samples was discussed,[12,13] but the effect of variation of Cd content at the expense of Ge content on the optical properties of thin films of this system was rarely studied. Therefore, we investigated the effect of the variation of Cd content in Se-Ge-Cd_x thin films on its optical properties.

(Received February 18, 2014; accepted March 18, 2016; published online April 12, 2016)

Thin films of $Se_{80}Ge_{20-x}Cd_x$ ($0 \le x \le 12$ at.%) were prepared by a thermal evaporation technique. The optical properties of the prepared films were studied. The transmission spectra measured by spectrophotometer (JASCO V-650) in the wavelength ranges (350 nm to 2500 nm) were used to determine the optical constants of the studied films. The refractive index of thin films was investigated Swanepoel's method.[14] An analysis of the refractive index results was carried out to obtain the high-frequency dielectric constant ε_∞ and other related parameters. An analysis of the absorption coefficient was carried out on the basis of Tauc's extrapolation procedure[15] in order to obtain the optical band gap E_g^{opt} and the nature of the involved optical transitions.

EXPERIMENTAL TECHNIQUE

$Se_{80}Ge_{20-x}Cd_x$ ($0 \le x \le 12$ at.%) compositions were synthesized in a bulk form by the well-known melt quenching technique. The elementary constituents of each composition of purity 99.999% were weighted in accordance with their atomic percentage (5 g total weight), loaded in silica tubes and then sealed under vacuum of (10^{-5} Torr). Each tube was placed in an oscillatory furnace and heated stepwise by a rate 5 deg/min up to 1223 K and kept constant for 24 h to ensure the homogeneity of composition. Then, each ampoule was quenched in icy, cold water to obtain the synthesized material in the amorphous state.

Thin films of the different compositions of $Se_{80}Ge_{20-x}Cd_x$ ($0 \le x \le 12$ at.%) were prepared by the thermal evaporation technique under vacuum (10^{-5} Torr) from molybdenum boats at a constant rate onto dry, cleaned, glass substrates using a coating unit (Edward E306A). The substrate was kept at room temperature during deposition. The film thickness of the as-prepared films are in range (200 nm to 620 nm), which were measured after evaporation by Tolansky's interferometric method.[16]

The chemical compositions of the investigated samples were determined by energy dispersive x-ray analysis (EDX) using a JOEL 5400 scanning electron microscope. Fully quantitative analysis results were obtained from the spectra by processing the data through a ZAF correction program. X-ray diffraction (XRD) reveals the amorphous nature of the investigated film compositions as shown in Fig. 1. The optical transmittance $T(\lambda)$ of the studied thin film samples were measured at room temperature, using unpolarized light at normal incidence by means of a double-beam spectrophotometer (Type JascoV-570). A scanning wavelength range of 350 nm to 2500 nm was utilized in steps of 2 nm.

RESULTS AND DISCUSSION

Structure Identification of $Se_{80}Ge_{20-x}Cd_x$ ($0 \le x \le 12$ at.%) glasses

XRD patterns of $Se_{80}Ge_{20-x}Cd_x$ ($0 \le x \le 12$ at.%) films are shown in Fig. 1. which contains a film pattern of each composition as a representative example. The spectra indicate an amorphous state which was the case for all films under investigation. The structure of films deposited on substrates at room temperature is expected to be amorphous because in the deposition process,[17] the evaporated molecules precipitate randomly on the surface of the substrate, and the following molecules also condense and adhere randomly, leading to film disordering. The same behavior was obtained for all other films of the studied compositions.

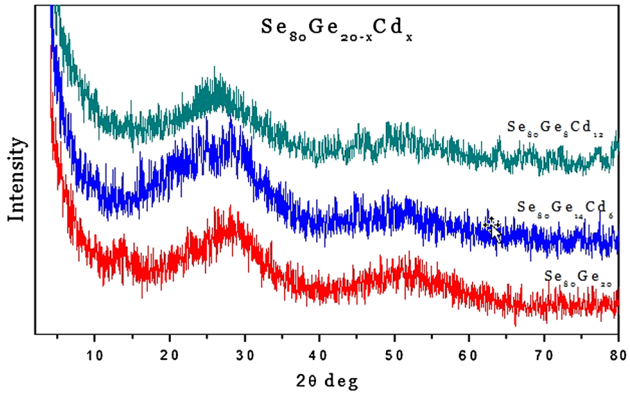

Fig. 1. X-ray diffraction patterns for the as-prepared $Se_{80}Ge_{20-x}Cd_x$ (x = 0, 6 and 12 at.%) thin films.

The amorphous structure of the deposited films on substrates kept at room temperature is expected because in the deposition process, the evaporated molecules precipitate randomly on the surface of the substrate and all the following condensed molecules adhere randomly leading to disordered films of increased thickness. The loss of adequate kinetic energy for the precipitated molecules keeps them unable to orient themselves to produce the chain structure required for the crystalline structure. The internal stresses required of the hot molecules on the cold, pre-deposited layers increase both the disorder and the degree of randomness, which yields amorphous films whatever their thickness is.

Calculation of the Refractive Index and Film Thickness

The measured transmittance data of the deposited $Se_{80}Ge_{20-x}Cd_x$($0 \le x \le 12$ at.%) films of nearly the same thickness (600 nm) are shown in Fig. 2, and those with different thicknesses are shown in Fig. 3a to c, for all the studied film compositions as examples, and we calculate the parameters by using one thickness (600 nm). It is clear from these figures that at the absorption edge, the interference fringes gradually disappeared, and all spectra show a sharp falling of transmittance derived from the fundamental absorption of the films. An excellent surface quality and homogeneity of the film were confirmed from the appearance of interference fringes in the transmission spectra[18,19] occurring when the film surface is reflecting without much

scattering/absorption in the bulk of the film.[20] Generally, outside the region of fundamental absorption ($h\nu > E_g$) or of the free-carrier absorption (for higher wavelengths), the dispersion of the refractive index, n and extinction coefficient, k, are not very large.

The optical constants (n and k) were evaluated using the Swanepoel method,[21] originally developed by Manifacier et al.[22]

If we assume that the film is weakly absorbing and the substrate is completely transparent, the refractive index, n, was calculated from the transmission spectrum using Swanepoel's method. In accordance with this method, the transmission spectrum can be subdivided into three distinct regions: (i) weak absorption region ($\lambda > 860$ nm), (ii) medium absorption region (670 nm $< \lambda <$ 860 nm), and (iii) strong absorption region (500 nm $< \lambda <$ 670 nm). Weak and medium regions of the spectrum have been used to determine refractive index, n, as a function of wavelength, λ, using the envelopes method.[21] Approximate initial values of the refractive index, n_i, for the $Se_{80}Ge_{20-x}Cd_x$ thin films, in the spectral region of medium and weak absorption, can be calculated by the following expression[21]:

$$n_i = \sqrt{[M + (M^2 - n_s^2)^{1/2}]}, \qquad (1)$$

where

$$M = 2n_s \frac{T_M - T_m}{T_M T_m} + \frac{n_s^2 + 1}{2}$$

Here, T_M, T_m are transmission maximum and the corresponding minimum at a certain wavelength λ; alternatively, one of these values is an experimental interference extreme and the other one is derived from the corresponding envelope and n_s (= 1.52) is the refractive index of the substrate. The approximate values of the refractive index can be employed to determine the film thickness as:

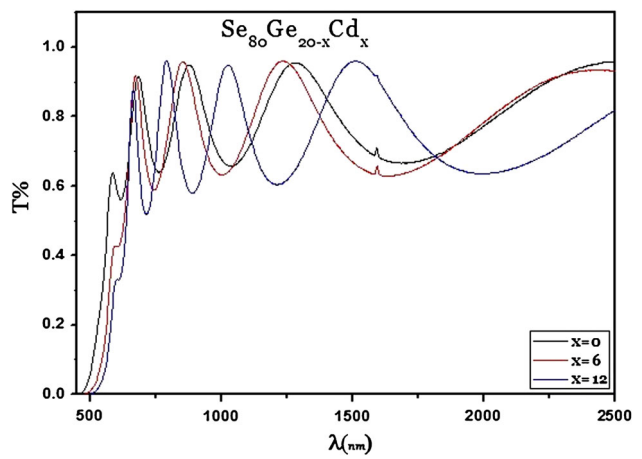

Fig. 2. Optical transmittance spectra of the evaporated $Se_{80}Ge_{20-x}Cd_x$ films.

$$t_i = \frac{\lambda_1 \lambda_2}{2(\lambda_1 n_2 - \lambda_2 n_1)} \qquad (2)$$

where n_1 and n_2 are the refractive indices at two adjacent maxima (or minima) at λ_1 and λ_2. The average value of t_1 ($\bar{t}_1$) was calculated from the low-deviation values, ignoring the highly deviated ones. The order number, m, of extremes could be calcu-

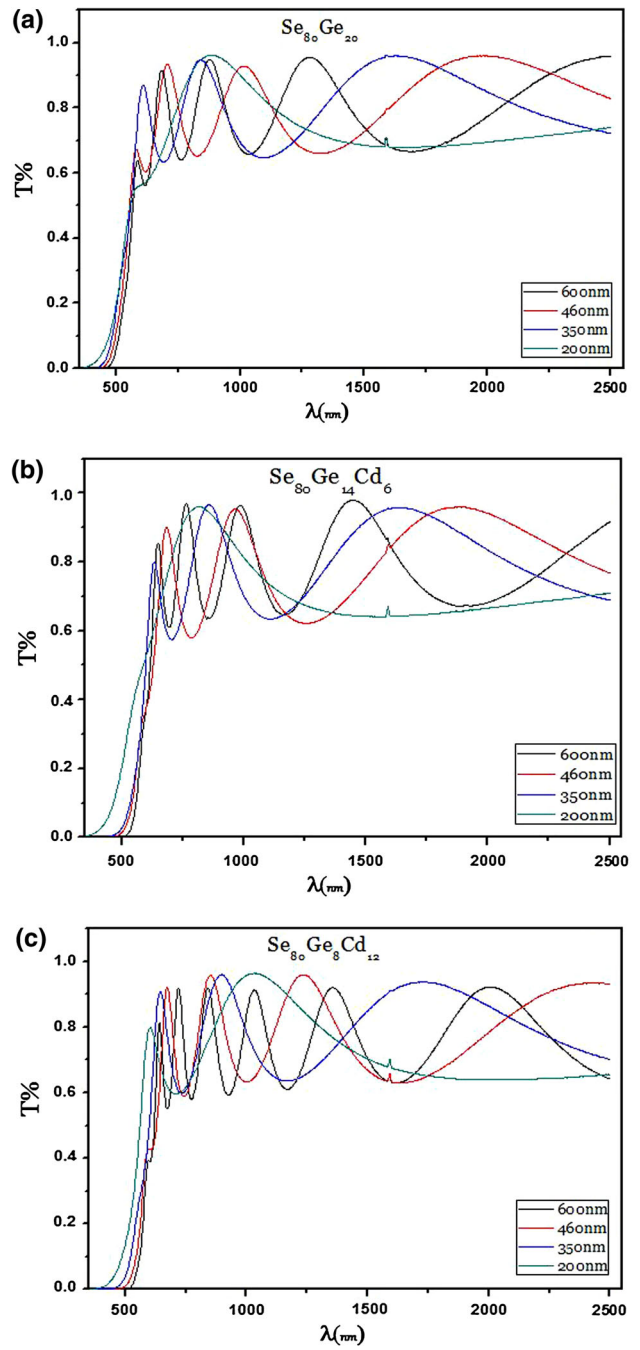

Fig. 3. (a) Optical transmittance spectra of the evaporated $Se_{80}Ge_{20}$ film. (b) Optical transmittance spectra of the evaporated $Se_{80}Ge_{14}Cd_6$ film. (c) Optical transmittance spectra of the evaporated $Se_{80}Ge_8Cd_{12}$ film.

lated from n and ($\bar{t}_1$) using the basic relation $2nt = m\lambda$, where m is an integer for maxima and a half integer for minima. Taking the exact values of m for each λ and calculating the thickness t_2 using the values of n again, an average thickness ($\bar{t}_2$) with suitable accuracy could be calculated. The calculated values of the thickness for the investigated films with x = 0, 6 and 12 at.% are ≈600 ± 20 nm, and they are found to be in reasonable agreement with that obtained from the Tolansky's interferometric method.[16] Using the accurate values of m and ($\bar{t}_2$), n can again be calculated for each λ. The calculated values of n, with an experimental error ±0.005, were found to fit a two-term Cauchy formula[23]:

$$n = a + b/\lambda^2 \tag{3}$$

with a correlation coefficient ~0.98. The n values at shorter wavelengths were estimated from the extrapolation of the fitted relation which as shown in the inset of Fig. 4. The estimated constant values a and b for $Se_{80}Ge_{20-x}Cd_x$($0 \le x \le 12$ at.%) films are summarized in Table I.

Figure 4 shows the spectral variation of the refractive index, n, for the investigated film compositions; the symbols represents the experimental set values of n obtained using the envelope method while the solid line represent the theoretical values of n calculated using the two-term Cauchy dispersion relation. It is clearly seen that both the experimental and calculated values of the refractive index for all the investigated samples are in extension to each other.

Since the values of the refractive index are already known over the spectral region studied, the absorbance ξ in the region of fundamental edge can be calculated using the formula suggested by Swanepoel[14]:

$$\xi = \frac{(n+1)^3(n+s^2)}{16n^2s}T_o, \tag{4}$$

where T_o is the recorded transmission data in fundamental edge. Using Eq. 4, one can get the absorption coefficient α in the form:

$$\alpha = -\ln(\xi/t), \tag{5}$$

Hence, the extinction coefficient, k that completes the derivation of the two optical constants (n, k) can be calculated using the well-known relationship;

$$k = \alpha\lambda/4\pi, \tag{6}$$

The calculated values of the absorption index k are plotted versus λ over the entire studied spectral range and are illustrated in Fig. 5 for the investigated film compositions. Figures 4 and 5 show that the values of n and k decrease with increasing the wavelength through the investigated range. The decrease in the refractive index is due to increase in the transmittance with the wavelength and decrease of absorption coefficient with wavelength. It is also evident from Fig. 4 that with the increase of Cd content, n increases. This increase is related to the increased polarizability of the large Cd atomic radius of 1.55 Å compared with that of Ge (1.22 Å).

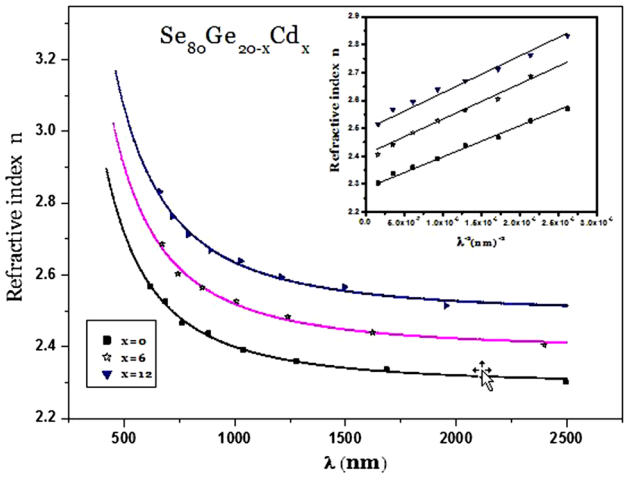

Fig. 4. Variation of the refractive index n for $Se_{80}Ge_{20-x}Cd_x$ film compositions.

Table I. The constant a and b values of the two-term Cauchy dispersion relation for the investigated samples

Composition	B ($\times 10^5$)	a
$Se_{80}Ge_{20}$	1.06	2.3
$Se_{80}Ge_{14}Cd_6$	1.3	2.4
$Se_{80}Ge_8Cd_{12}$	1.43	2.5

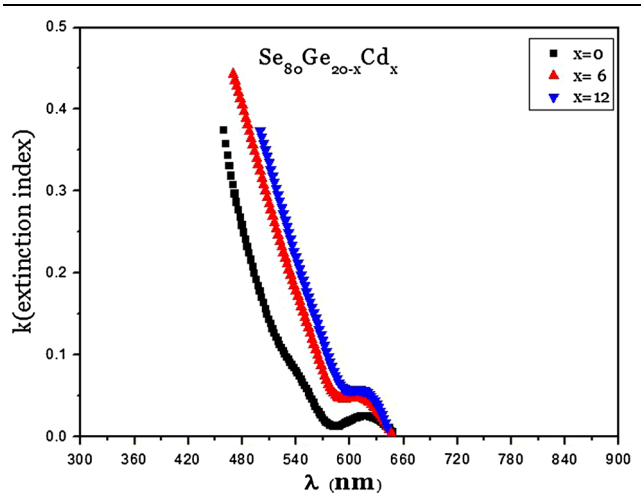

Fig. 5. Dependence of the extinction index k on wavelength λ for $Se_{80}Ge_{20-x}Cd_x$ films.

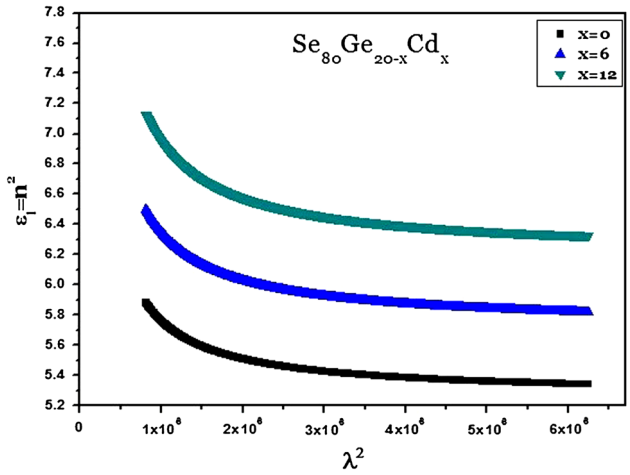

Fig. 6. Plot of n^2 versus λ^2 for $Se_{80}Ge_{20-x}Cd_x$ film.

Analysis of the Refractive Index Data

The complex dielectric constant, ε^* of a material is given in terms of the real, n and imaginary k parts of the complex refractive index, n^* as: $\varepsilon_1 = n^2 - k^2$, where ε_1 is the real part of the complex dielectric constant and $\varepsilon_2 = 2nk$ is the imaginary part. In the transparent region ($k \approx 0$), the real part of the dielectric constant can be written as[24]:

$$\varepsilon_1 = \varepsilon_{\infty L} - \beta\lambda^2, \tag{7}$$

where $\beta = \frac{e^2 N}{4\pi^2 c^2 \varepsilon_o m^*}$; and $N/m^* = \frac{\varepsilon_o \varepsilon_{\infty L}}{e^2}\omega_p^2$, where $\varepsilon_{\infty L}$ is the lattice dielectric constant, c is the velocity of light, ε_o is the free space dielectric constant, e is the electronic charge and N/m^* is the ratio of the carrier's density to the free carrier effective mass and ω_p is the plasma frequency corresponding to the valence electrons involved in the optical transitions.

A plot of the square of the refractive index n^2 versus λ^2 according to Eq. 7 is shown in Fig. 6. It is observed that the dependence of n^2 on λ^2 is linear at longer wavelengths. Extrapolating the linear part of this relation, the zero wavelength gives the values of $\varepsilon_{\infty L}$, given in Table II for the investigated compositions. The ratio N/m^* was calculated from the slope of the linear part of n^2 versus λ^2 relation (Fig. 6) and the obtained values given in Table II are used to calculate the plasma frequency ω_p. The obtained values of N/m^*, ω_p, $\varepsilon_{\infty L}$ and the lattice refractive index, $(n_L = \sqrt{\varepsilon_{\infty L}})$ are also given in Table II. It is seen that the value of N/m^* reflects to increases in the free carrier density with the increase of Cd content.

The spectral dependence of the refractive index data n (λ) was further analyzed using the Wemple–DiDomenico (WDD) model,[25,26] based on the single-oscillator approach in the region from the visible to near-infrared having the following equation:

$$\varepsilon_1(\omega) = n^2 - 1 = \frac{E_o E_d}{E_o^2 - (\hbar\omega)^2}, \tag{8}$$

Table II. The parameters $\varepsilon_{\infty L}$, N/m^*, ω_p and n_L for the investigated films

Composition	$\varepsilon_{\infty L}$	N/m^* (m^3 kg^1)	ω_p (s^{-1})	n_L
$Se_{80}Ge_{20}$	5.74	1.81×10^{56}	3.02×10^{14}	2.39
$Se_{80}Ge_{14}Cd_6$	6.23	2.83×10^{56}	3.62×10^{14}	2.56
$Se_{80}Ge_8Cd_{12}$	6.87	4.1×10^{56}	4.1×10^{14}	2.62

where $\hbar = h/2\pi$ (h is Planck's constant), ω is the frequency and E_o *is* the single oscillator energy and E_d is the oscillator strength, which is a measure of the interband optical transitions. The E_o and E_d parameters are determined by plotting $(n^2 - 1)^{-1}$ versus $(\hbar\omega)^2$ for the investigated compositions and by fitting a straight line to the smaller energy data as shown in Fig. 7; the slope = $(E_o E_d)^{-1}$ and the intercept on the vertical axis = E_o/E_d. The single oscillator parameters E_o and E_d are calculated using these two relations and are listed in Table III. The parameter E_d and E_o are also used to calculate the static refractive index ($n_s(0)$) (where $n_s(0) = \sqrt{1 + E_d/E_o}$), static high frequency dielectric constant, ε_s, ($\varepsilon_s = (n_s(0))^2$) and the Wemple–DiDmenico band gap $E_g^{W.D} = E_o/2$.[26] The estimated values of E_o, E_d, $n_s(0)$, ε_s and $E_g^{W.D}$ are given also in Table III as a function of Cd content. The data reported in Table III demonstrates that the value of the calculated refractive dispersion parameters decreases as the Cd increases. It was also seen that the obtained static refractive index, n_s and the Wemple–DiDmenico band gap, $E_g^{W.D}$ are comparable with the constant 60 obtained from the empirical relation suggested by Moss[27] which relates the refractive index, n, to the optical band gap value E_g;

$$n^4 E_g = 60, \tag{9}$$

It is worth mentioning here that the advantage of using the single oscillator equation (Eq. 8) to fit the refractive index data is that it provides intuitive physical interpretations of the measured quantities. In particular, the average gap, E_o, gives quantitative information on the overall band structure of the material. The parameter E_o known as WDD gap corresponds to the distance between centers of gravity of the valence and conduction bands. Therefore, it is related to the average bond strength or the cohesive energy of the systems. Since the average heat of atomization $\langle H_s \rangle$, whose values are given in Table III, is defined for a system as a direct measure of the cohesive energy (CE) and thus of the average bond strength,[28] therefore, the increase in Cd content with lower bond energy than other bonds increases the weaker bond density in the studied composition and leads to lowering the average bond energy and, hence, the CE of the system. This is quite different from the information coming from

the value of the optical gap, E_g^{out}, which probes the optical properties near the band edges of the material. It is also related to the average bond strength of the system.

Analysis of Absorption Coefficient α

Study of the optical absorption of materials provides a simple method for explaining some features concerning the band structure and energy gap of non-metallic samples.

The absorption coefficient of the investigated film samples is calculated according Eq. 6, as mentioned above, for different values of wavelength in the considered spectrum range. For many amorphous materials, the absorption edge can be divided into two regions depending on the value of the absorption coefficient (low- and high-energy absorption regions).[29] Figure 8 shows the dependence of the absorption coefficient, α, on photon energy, $\hbar\omega$, for the deposited $Se_{80}Ge_{20-x}Cd_x$ films. It is observed that the optical absorption spectra show two distinct absorption regions:

1. Low-energy absorption region in the photon energy range 1.88 eV to 2.1 eV, at which the magnitude of the optical absorption coefficient $\alpha < 10^4$ cm^{-1}, there is an Urbach tail.[30] The absorption coefficient can be described by the relation.

$$\alpha(\hbar\omega) = \alpha_o \exp(\hbar\omega/E_e), \qquad (10)$$

where α_o is constant in general and E_e is the width of the band tail of the localized states at the optical band gap and represents the degree of disorder in amorphous semiconductor materials.[15] Figure 9 illustrates the variation of lnα with photon energy and the value of E_e can be evaluated according to Eq. 10. The width of the localized state tails at the band gap E_e can be calculated from the plots of ln α versus $\hbar\omega$ according to Eq. 10. The experimental data shown in Fig. 9 indicate a good fit with the exponential of Eq. 10. The reciprocal of the slope yields the value of E_e, while the intercept gives α_o values. The obtained values of E_e and α_o are given in Table III.

Variations in the width of the exponential region E_e provide information about the relative changes of the structure disorder in amorphous semiconductors. For a good chalcogenide material, a typical value of E_e is around 50 meV. Tauc[15] believed that it arises from electronic transitions between localized states in the band edge tails where the density of localized states is exponentially dependent on energy. Davis and Mott were uncertain about the precise explanation of the dependence and suggested that the slopes of the observed exponential edges obtained from the above equation are the same in many semiconductors, and the values of E_e for a range of

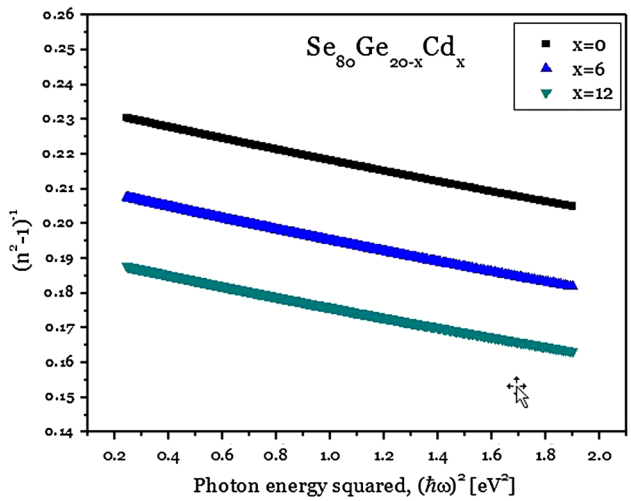

Fig. 7. Plots of $(n^2 - 1)^{-1}$ versus $(h\nu)^2$ for $Se_{80}Ge_{20-x}Cd_x$ films.

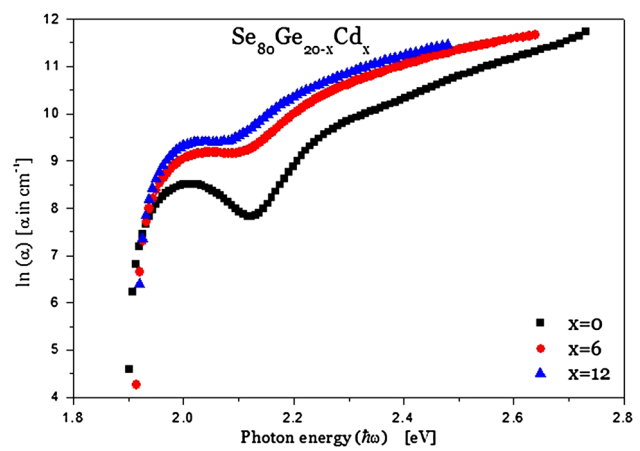

Fig. 8. Spectral variation of the absorption coefficient, α, versus photon energy.

Table III. Values of the Wemple–DiDmenico oscillator parameters and E_e, α_o and E_g^{opt} for $Se_{80}Ge_{20-x}Cd_x$ thin films

Sample	E_d (eV)	E_o (eV)	$n_s(0)$	ε_s	E_g^{WD} (eV)	$n_s^4 E_g^{W.D}$	E_e (meV)	α_o (cm^{-1})	$E_g^{ind.}$ (eV)
$Se_{80}Ge_{20}$	16.4	3.861	2.296	5.274	1.931	53.7	47	7.5×10^{-16}	2.07
$Se_{80}Ge_{14}Cd_6$	17.3	3.66	2.395	5.74	1.83	60.12	56	3.7×10^{-12}	1.92
$Se_{80}Ge_8Cd_{12}$	18.6	3.56	2.496	6.23	1.78	69.02	59	1.65×10^{-11}	1.87

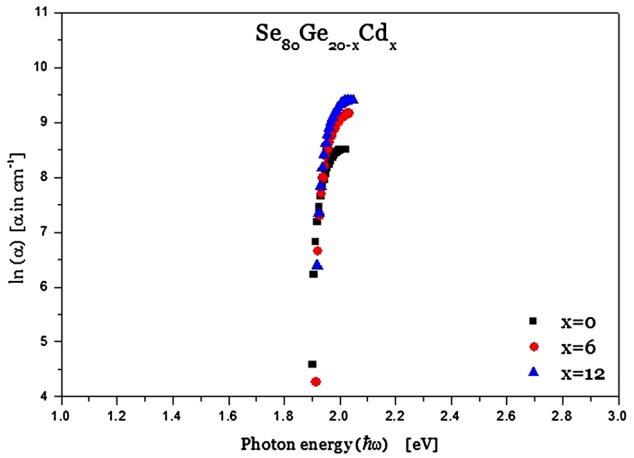

Fig. 9. Plot of ln*a* versus photon energy $\hbar\omega$.

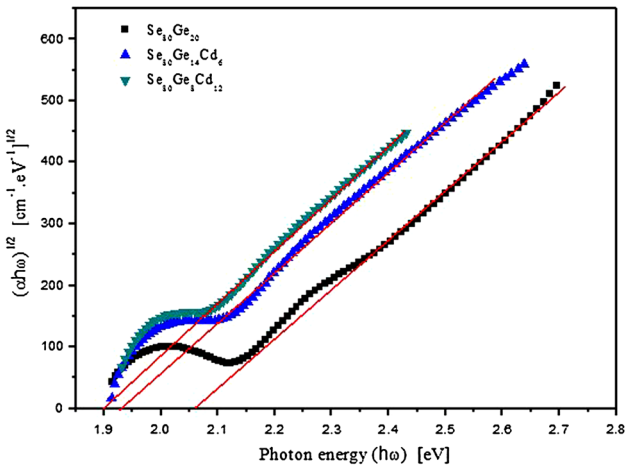

Fig. 10. Absorption coefficient plotted as $(\alpha\ \hbar\omega)^{1/\gamma}$ versus $\hbar\omega$ for $Se_{80}Ge_{20-x}Cd_x$ films.

amorphous semiconductor materials lie between 0.045 eV and 0.67 eV.[31]

2. The high absorption region in the photon energy range 2.1 eV to 2.7 eV, where the magnitude of the optical absorption coefficient $\alpha > 10^4$ cm^{-1}, corresponds to transitions between states in both valence and conduction bands, where the optical absorption coefficient, α, for the studied films obeys the following relation[30]

$$\alpha(\hbar\omega) = A(\hbar\omega - E_g^{opt})^{\gamma}, \qquad (11)$$

where, A is a constant arising from Fermi's golden rule for fundamental electronic transitions within the framework of parabolic approximation for the dispersion relation, and E_g^{opt} is the optical band gap of the material. The exponent γ is an index parameter, which characterizes the type of the optical transition and is theoretically equal to 2, 1/2, 3 or 3/2 for indirect allowed, direct allowed, indirect forbidden and direct forbidden transitions, respectively. The usual method to know the type of the optical transition and determine the corresponding energy value involves a plotting of$(\alpha\hbar\omega)_{1/\gamma}$ versus $\hbar\omega$ in accordance to Eq. 11 as shown in Fig. 10. This figure shows that the plot is a linear function, and this linearity revealed that the existence of allowed indirect optical transitions successfully describes the transition mechanism in the studied films. The intercept of the extrapolation of the linear part to zero absorption with the photon energy axis is taken as the value of the forbidden energy gap E_g^{opt}. Values of the optical band gap for $Se_{80}Ge_{20-x}Cd_x$ (x = 0, 6 and 12 at.%) films are listed also in Table III.

From the above analysis it is indicated that the optical energy gap E_g^{opt} decreases with increasing Cd content at the expense of Ge content (see Table III). The obtained values of E_g^{opt} for the studied compositions are found to decrease from 2.07 eV to 1.87 eV. This may be due to the fact that[32] chalcogenide glasses have greater compositional disorder. In amorphous materials, the band edges are broadened mainly by the lake of long range order as well as by the presence of defects. It is also evident from Table III that the band tailing parameter E_e increases with increasing Cd content which may be due to the formation of structural defects. The concentration of these defects increases with Cd content. Therefore, these defects can introduce localized states at or near the band edges leading to an increase in the disorder of the system and increasing the band tailing width.[30,33,34] The decrease in the optical energy gap could be also discussed on the basis of density of states model proposed by Mott and Davis.[35] Chalcogenide films always contain a high concentration of unsaturated bonds or defects. These defects are responsible for the presence of localized states in the amorphous band gap. On the other hand, the nature of the chemical bonds present in the system can have some effect on the obtained values of E_g^{opt}. The bond energy values have been calculated on the basis of the relation[36]:

$$D(A-B) = (D(A-A) \times D(B-B))^{\frac{1}{2}} + 30(\chi_A - \chi_B)^2 \qquad (12)$$

where χ_A and χ_B are the electro negativities of the A and B, and $D(A\text{-}A)$ and $D(B\text{-}B)$ are the bond energies of A-A and B-B bonds, respectively. The calculated

Table IV. The bond energy of elements

Bond	Bond energy (kJ/mol)
Ge-Se	206.7
Cd-Se	177
Ge-Ge	157.2
Ge-Cd	141.38
Cd-Cd	127.1
Se-Se	184.1

results are given in Table IV, from which it is clear that Ge-Cd and Ge-Ge bond energies are weaker than Se-Ge and Se-Cd bond energies. This results in lowering the average bond energy of the studied glasses by the increase of Cd content. Thus, the increase of Cd content will decrease the optical energy gap values as a result of increasing the weaker bonds and, hence, in lowering the average bond energy of the investigated compositions.

CONCLUSIONS

Thin films of amorphous $Se_{80}Ge_{20-x}Cd_x$ ($0 \le x \le 12$ at.%) chalcogenide glasses were prepared by a thermal evaporation technique. X-ray analysis predicts the amorphous nature of the prepared films for all studied compositions.

Optical characterization of $Se_{80}Ge_{20-x}Cd_x$ ($0 \le x \le 12$ at.%) thin films have been analyzed based on the generation of the envelopes of the interference maxima and minima of the transmission spectrum (Swanepoel's method). Transmittance $T(\lambda)$ measurements in the spectral range 350 nm to 2500 nm were used to calculate the optical constants (n and k), the optical band gap E_g^{opt} and the width of localized states E_e. Analysis of the refractive index data according to the single oscillator model results in the dispersion parameters (E_d, E_o, $\varepsilon_{\infty L}$ and N/m^*). The optical absorption measurements indicated that the absorption mechanism is due to allowed indirect transmissions. The optical energy gap E_g^{opt} decreases with increasing Cd content. The decrease in E_g^{opt} may be due to the increase of the disorder in the investigated film samples as a result of increasing E_e and leads to an increased density of the localized states in the mobility gap.

The absorption coefficient α increases with increasing Cd content. The increase in α indicates that the charge carriers absorb more energy. A large absorption coefficient and the compositional dependence of other parameters make these materials suitable for optical data storage.

ELECTRONIC SUPPLEMENTARY MATERIAL

The online version of this article (doi: 10.1007/s11664-016-4470-0) contains supplementary material, which is available to authorized users.

REFERENCES

1. A.B. Seddon, *J. Non-Cryst. Solids* 184, 44 (1995).
2. B. Bureau, X.H. Zhang, and F. Smektala, *J. Non-Cryst. Solids* 345, 276 (2004).
3. J. Hu, V. Tarusov, A. Agrarwal, L. Kimerling, N. Carlie, L. Petit, and K. Richardson, *Opt. Express* 15, 2367 (2007).
4. A. Zakery and S.R. Elliott, *J. Non Cryst.* 330, 1 (2003).
5. T. Wanger, M. Kibal, J. Jedelsky, M. Vilcek, B. Frumarova, and M. Frumar, *J. Optoelectron. Adv. Matter.* 7, 153 (2005).
6. M. Frumar, J. Jedelský, B. Frumarová, T. Wágner, and M. Hrdlička, *J. Non-Cryst. Solids* 326–327, 399 (2003).
7. J.M. Gonzalez-leal, P. Krecmer, J. Prokop, and S.R. Elliott, *J. Non-Cryst. Solids* 326–327, 416 (2003).
8. M.A. Mageed Khan, M. Zulfequar, and M. Hussain, *J. Phys. Chem. Solids.* 62, 1093 (2001).
9. I. Sharma, S.K. Tripathi, and P.B. Barman, *J. Phys. D: Appl. Phys.* 4, 4460 (2007).
10. H.E. Atyia, N.A. Hegab, M.A. Afifi, and M.I. Ismail, *J. Alloys Compd.* 574, 345 (2007).
11. H.E. Atyia and N.A. Hegab, *Eur. Phy. J. Appl. Phys.* 63, 10301 (2013).
12. R.K. Shukla, S. Swarup, A.K. Agnihotri, A.N. Nigam, and A. Kumar, *J. Philos. Mag. Lett.* 63, 165 (1991).
13. M.R. Balboul, *J. Phys. B* 434, 78 (2014).
14. R. Swanepoel, *J. Phys. E, Sci. Instrum.* 17, 896 (1984).
15. J. Tauc, *Optical Properties of Solids* (Amsterdam: North Holland, 1970), p. 903.
16. A. Tolansky, *Introduction to Interferometry* (NewYork: Longman, 1951).
17. N.A. Hegab, I.S. Yahia, A.M. Shakra, A.E. Bekheet, and A.M. Al-Ribaty, *J. Alloy Compd.* 509, 5935 (2011).
18. R. Swanepoel, *J. Phys. E: Sci. Instrum.* 16, 1214 (1983).
19. L. Bhira, H. Essaidi, S. Belgacem, G. Couturier, J. Salardenne, N. Barreau, and J.C. Bernede, *Phys. Status Solidi (a)* 181, 427 (2000).
20. J. George, K.S. Joseph, B. Pradeep, and T.I. Palson, *Phys. Status Solidi (a)* 106, 123 (1988).
21. A.H. Moharram, A.A. Othman, H.H. Amer, and A. Dahshan, *J. Non-Cryst. Solids* 352, 2187 (2006).
22. J.C. Manifacier, J. Gasiot, and J.P. Fillard, *J. Phys. E.* 9, 1002 (1976).
23. T.S. Moss, *Optical Properties of Semiconductors* (London: Buttenworths, 1959).
24. T.S. Moss, G.J. Burrell, and E. Ellis, *Semiconductor Opto-Electronics* (London: Butterworth, 1973).
25. G. Kumar, J. Thomas, N. George, B. Kumar, P. Shnan, V. Npoori, C. Vallabhan, and N. Unnikrishnan, *Phys. Chem. Glasses* 41, 89 (2001).
26. S.H. Wemple and M. DiDomenico, *Phys. Rev. B.* 3, 1338 (1971).
27. S.H. Wemple, *Phys. Rev. B.* 7, 3767 (1973).
28. V. Sadagopan and H.C. Gatos, *Solid State Electron.* 8, 529 (1965).
29. A.E. Owen, A.P. Firth, and P.J.S. Ewen, *Philos. Mag. B* 52, 347 (1985).
30. F. Urbach, *Phys. Rev. B.* 92, 1324 (1953).
31. E.A. Davis and N.F. Mott, *Philos. Mag.* 22, 903 (1970).
32. N.A. Hegab and H.M. El-Mallah, *Phys. B* 407, 33 (2012).
33. M. Itayas, M. Zulfequar, and M. Husain, *J. Mod. Opt.* 47, 663 (2000).
34. T.T. Nang, M. Okudo, T. Matsushita, S. Yokota, and A. Suzuki, *Jpn. J. Appl. Phys.* 4, 849 (1976).
35. N.F. Mott and E.A. Davis, *Electronic Processes in Non-crystalline Materials* (Oxford: Clarendon, 1979), p. 428.
36. L. Pauling, *The Nature of the Chemical Bonds*, 3rd ed. (New York: Cornell University Press, 1960).